Validation of Computation Tools for Helium Cooling in ESS Target Station

Per Nilsson, Pascal Sabbagh, Cyril Kharoua and Yong Joong Lee
European Spallation Source ESS AB, Lund, Sweden

E-mail: per.nilsson@esss.se

Abstract.
The ESS spallation target station will be taking 5 MW from the proton beam, generating heat that has to be removed. A number of subsystems of the ESS target station will, according to the current baseline, be cooled by non-cryogenic helium gas. The considered helium cooling methods include both active circulation and natural convection.

The prediction of the target station subsystem cooling by helium flow using advanced 3D CFD simulation technologies takes a large part in the design efforts. Computational tools for 3D flow simulations are provided by ANSYS-Fluent/CFX, STAR-CD, OpenFOAM, and others. While these tools are extensively verified and validated by a large number of benchmark studies for gas flows composed of air or steam, only a limited number of validation cases are existing for gas properties of helium.

In this paper, two CFD simulation validation studies are presented for gas flow. ANSYS-Fluent has been used as a primary tool for the validation studies, supplemented by ANSYS-CFX. The reference experimental data for the simulation benchmarks are taken from the literature. The first validation case consists of a vertical annular section heated from the inside, where physical aspects of natural convection in nitrogen and helium gas are studied. The heat transfer via thermal radiation is also taken into account by Discrete Ordinates (DO) method. It is shown that the numerical methods are able to predict the heat transfer to a reasonable accuracy. Here, the radiative heat transfer becomes more dominant than the natural convection in that the accurate modeling of the surface emissivity appears to play a more important role than the modeling of the turbulence. The second validation case consists of a narrow heated channel with air flow. For the studied experimental flow setup, the flow was observed to go from turbulent flow to laminar. It is shown that the numerical methods are able to predict such laminarization, to a certain extent.

1. Introduction

The spallation target at ESS must withstand the very high intensity proton beam with time-averaged power of up to 5 MW. A large amount of heat will thus be generated in the target station. While many of the target subsystems will be cooled by conventional water circuits, a number of subsystems exposed to radioactive contamination are planned to be cooled by helium gas flow, either by active forced convection or by passive natural convection. These subsystems include the rotating tungsten target system and several components within the monolith surrounding the target-moderator system, such as the proton beam window. Among these, the cooling of the target gets particular attention due to its tough operating conditions.

The present ESS baseline design of the rotating target is composed of tungsten blocks that are contained in a stainless steel shroud of radius 2.5 m. The target wheel rotates with the frequency

of $\mathcal{O}(0.5)$ Hz, in order to distribute heat load more uniformly around the circumference. The internal helium circuit for the target provides pressurized gas flow through the cooling channel between the tungsten blocks within the shroud. See [1] for further details. The target wheel is surrounded by helium with a pressure slightly less than atmospheric pressure. The external part of the target shroud will be cooled by radiative heat transfer and natural convection in this helium.

For the prediction of the operating temperature and the associated thermo-mechanical loads of the target systems, the CFD simulation tools must be able to capture the physics of thermal expansion, thermal compression, radial acceleration of the pressurized helium flow and the correct convective heat exchange between the helium flow and target material. In this paper, CFD analyses of chosen validation benchmark cases for gas low are presented.

The work presented here is a part of the continuously ongoing validation of computational tools. The purpose is to ensure the applicability of the calculations for the target station and to learn about the accuracy of this type of simulations. The goal is to investigate two cases with similarities with the target station applications and compare to measurements presented in the literature.

Two cases are investigated. The first case is a vertical annular section heated from the inside, including natural convection and radiation. The second case is a narrow heated channel, where the flow is on the border between turbulent and laminar flow. In this work, the modeling framework should be used as default as possible - that is without tuning, in order to mimic the usage for applications where there is no measurements to tune to. It is not intended to improve the modeling tools or make a direct comparison between them.

2. Validation Case 1: Natural convection and radiation

The strength of natural heat convection or "buoyantivity" depends on the physical properties of the fluid.

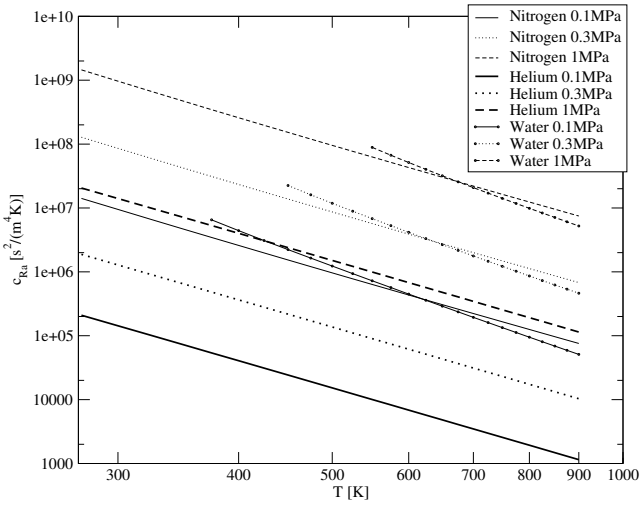

Figure 1. "Buoyantivity" parameter

The buoyantivity of different gases can be quantitatively described by the constant c_{Ra}, which is defined by the relation,

$$\mathsf{c}_{\mathrm{Ra}} = \frac{\beta}{\nu\alpha}, \tag{1}$$

where ν is the kinematic viscosity, β is the thermal expansivity and α is the thermal diffusivity. The buoyantivity parameter c_{Ra} is related to the dimensionless Rayleigh number,

$$Ra = g\,\mathsf{c}_{\mathrm{Ra}}\,(T_{\mathrm{wall}} - T_{\mathrm{free}})\,L^3, \tag{2}$$

which quantifies the strength of the natural heat convection.

In this section, a validation study is presented, evaluating the CFD tools for describing natural convection in helium gas. The benchmark case consists of a closed annulus that is heated from the inner surface and cooled from the outer surface. It also includes radiative heat transfer between the solid walls. The validation case and measurement data are taken from [2].

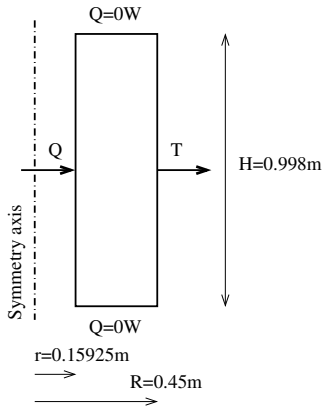

The annulus is modeled as a sector of a few degrees with symmetry conditions in the tangential directions. The inside of the annulus is electrically heated and the outside wall is water cooled; see Figure 2. At the inner radius, a constant heat flow rate is set in the model. At the outer radius, a constant temperature is set in the model. The inner (heated) surface has a constant emissivity of 0.7 and the outer (cooled surface) has an emissivity of 0.5. Both these values are taken from [2].

Figure 2. Buoyancy/radiation model

The air properties are modeled as follows with Fluent's built in functions: Density = ideal-gas, Specific Heat Capacity = piecewise-polynomial, Thermal Conductivity = kinetic-theory and Dynamic Viscosity = power-law. Turbulence is modeled based on RANS with $k-\omega$ SST. For radiation, the method of Discrete Ordinates (DO) is used with default Fluent settings. The mesh has 30 volumes in the radial direction and 50 in the axial direction, both with a bias of 10 refining the mesh towards the walls. Fluent's default settings are also used for schemes and solution control, except for the momentum relaxation which is increased from 0.7 to 0.2. The default first order schemes are considered sufficient for this case with small gradients. The solutions converge rather well with helium, but with nitrogen the residuals do not decrease as well. This could be due to that the natural convection in nitrogen is not stationary here, but remains to be investigated. Nevertheless, as will be shown below, the average results still compare rather well to the experiments.

The following figures and descriptions show the simulated and measured inner wall temperatures. In figure 3 to 5, the temperature is plotted along the axial=vertical direction for a total heating power of $14.6kW$ or a heat flux of $14.6kW/m^2$.

Figure 3 compares the simulated temperatures for different filling gases with the measured counterparts. The simulations and measurements show good agreement between $0.2m$ and $0.8m$. There are deviations at the adiabatic boundary regions at the top and at the bottom. At the top, above $0.8m$, the wall temperature tends to increase as the tangential component of the gas velocity decreases. The phenomenon is qualitatively well captured by the simulations, except for near to the boundary. At the bottom, below $0.2m$, the simulation does not capture the increasing wall temperature. This might be due to the fact that some of the details of the experimental setup are not modeled in the simulation model. The inner wall of the experiments is heated with a cylindrical heater which contains air on the inside, possibly leading to a heat distribution, whereas the simulations are made with a constant heat flux. Also, the outer wall of the experiments is cooled with water circuits, possibly leading to a heat distribution, whereas most of the simulations are made with a constant outer wall temperature.

Figure 4 compares the simulated and measured temperatures for the helium gas run. Here, the result obtained by a simulation with CFX is presented in addition to the one obtained with a Fluent setup. CFX is used with a slightly different setup. It has a somewhat more dense

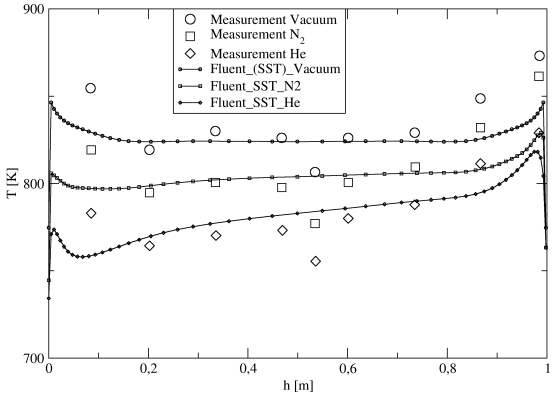

Figure 3. Inner (heated) wall temperature along vertical height for nitrogen, helium and vacuum

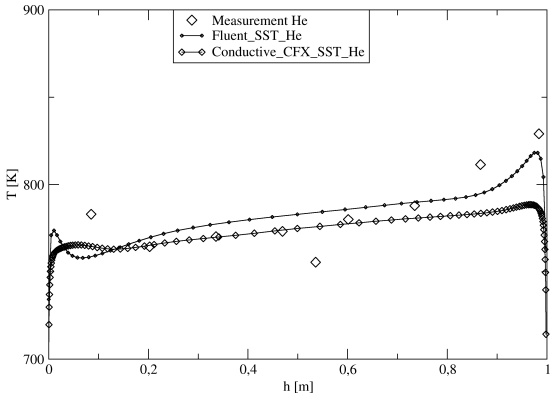

Figure 4. Inner (heated) wall temperature along vertical height for helium

mesh and uses a constant heat transfer coefficient with a bulk temperature on the outer wall. It also uses the P1 radiation model, which lacks directional information compared to the DO method. The CFX model captures the increasing wall temperature at the bottom region below $0.2m$ qualitatively. However, it shows poorer agreement with the experiment at the top region, above $0.8m$, than with Fluent. This might come from different boundary conditions used for different radiation model settings.

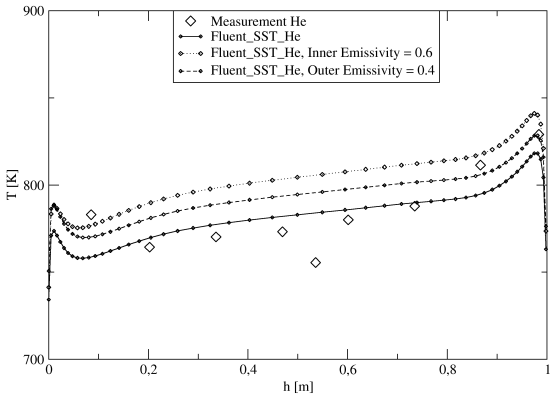

Figure 5. Inner (heated) wall temperature along vertical height for helium, testing emissivity

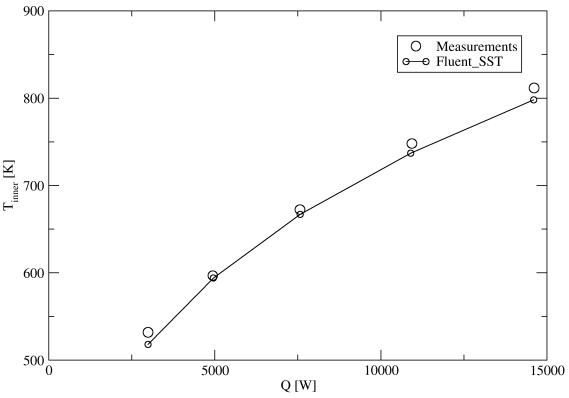

Figure 6. Mean inner (heated) wall temperature as a function of heating power for N_2

Figure 5 shows the effect of different internal wall surface emissivities, ε, on the simulated temperature fields. Three runs are considered, one with reference values ($\varepsilon_{\text{in}} = 0.7$ for the inner wall and $\epsilon_{\text{out}} = 0.5$ for outer wall), one with a lowered inner wall value ($\varepsilon_{\text{in}} = 0.6$ and $\varepsilon_{\text{out}} = 0.5$) and one with lowered outer wall value ($\varepsilon_{\text{in}} = 0.7$ and $\varepsilon_{\text{out}} = 0.4$). The simulations based on

reduced surface emissivities show increased wall temperatures. The impact of reducing ε_{in} is greater. This is due to the fact that the inner wall temperature is much higher than that of the outer wall.

Figure 6 shows a comparison between the simulated and measured mean inner wall temperatures, for different heat fluxes to the nitrogen filled volume and reference surface emissivity settings ($\varepsilon_{\text{in}} = 0.7$ and $\varepsilon_{\text{out}} = 0.5$). The reason for comparing for nitrogen is that these results are not presented for helium in Ref. [2]. The simulations and measurements show good agreement.

3. Validation Case 2: Channel heat transfer with laminarization

In order to investigate the modeling of heat transfer and the ability of the software tools to predict laminarization, a case with a heated channel is investigated. The measurement data are taken from [3] and [4]. This measured data has already been used for an investigation in depth of RANS turbulence models using STAR-CD in [5].

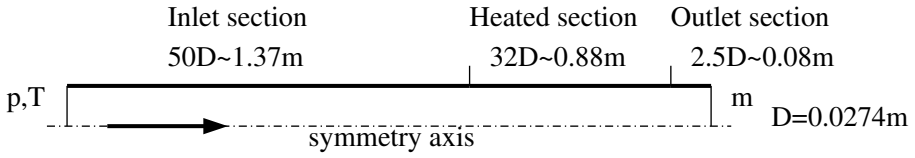

Figure 7. Simulation model for channel case (not to scale)

The 2D axi-symmetric model of the $D_i = 27.4mm$ pipe is described in Figure 7. Gauge pressure ($P_{in,gauge} = -8650Pa$) and temperature ($T_{in} = 297K$) are given at the pressure inlet boundary. The inlet turbulence intensity and length scale are set to 10% and $0.01m$ respectively. The mass flow rate at the outlet and the heat flux at the heated section are given according to Table 1. The wall roughness is set to 0 and for the outlet wall, the shear is also set to 0, in order to remove the artificial flat velocity profile of the boundary condition somewhat from the heated section. The reason for setting the pressure at the inlet is that it is not known at the outlet.

Table 1. Runs (The type names, characterising the flow, are taken from [4].)

Run	Mass flow rate $[g/s]$	Heat flux $[kW/m^2]$	Re_{inlet}	Type
618	2.39	2.1	6000	Turbulent
635	2.39	4.2	6000	Subturbulent
445	1.69	3.8	4000	Laminarizing

The air properties are set in the same way as for the natural convection and radiation case described above, that is with Fluent's built in functions. Turbulence is modeled in two ways based on RANS; with $k-\omega$ SST and $k-\epsilon$ Realizable, the latter with Non-Equilibrium Wall Functions. Special modeling of the transitional turbulence is also tested, based on extra transport equations for intermittency and transition momentuum thickness Reynolds number. This modeling is done with default settings. In the heated section, the volumes are $3.425mm$ long and in the inlet and outlet they are stretched towards the boundaries. In the radial direction, the bias parameter is 20, refining the mesh at the wall and the number of volumes vary according to Table 2. These fine surface resolutions are selected based on the results of [5]. Fluent's

Table 2. Radial mesh resolution.

No.	Radial volumes	Volumes	Wall y^+
mesh0	10	3680	1.1
mesh1	15	5520	0.7
mesh2	30	11040	0.4

default settings are used for schemes and solution control, except for the momentum relaxation which is increased from 0.7 to 0.3. The default first order schemes are considered sufficient, also for this case with small gradients. The solutions for run 618 are initialized with $U = 3m/s$, $P_{gauge} = -8650Pa$, $T_{in} = 297K$, default turbulence variables and run for 1200 iterations, where all residuals have stabilized at a low level. The solutions for runs 635 and 445, which are less numerically stable, are started from the solutions of run 618 and then run for 1200 iterations.

Figures 8 to 10 show axial distributions of temperature on the heated wall for the three runs respectively. Note that the vertical scales differ. It can be noted that the results differ a bit at the entrance and exit. This is likely due to axial heat transfer in the wall and outside in the experiments, which is not included in the simulations.

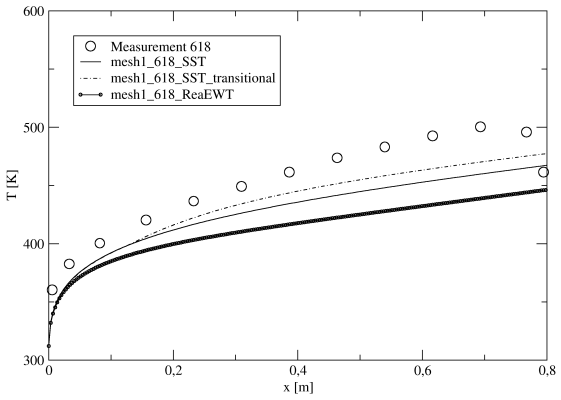

Figure 8. Heated wall temperature 618

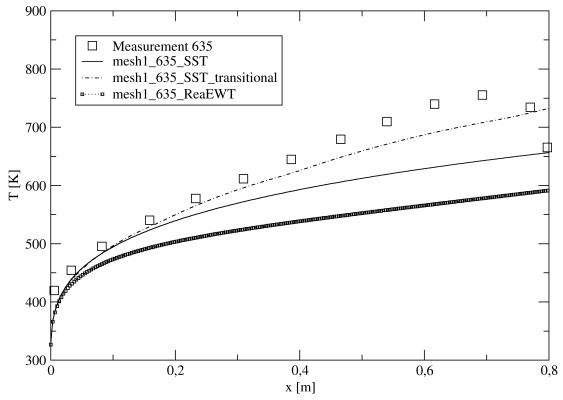

Figure 9. Heated wall temperature 635

In the turbulent run, 618, the match between the SST simulations and the experiments is reasonable. The transitional model gives a slight improvement, even if the flow is basically turbulent in this run.

In the so called subturbulent run, 635, the match between the SST simulations and the experiments is less good than for the turbulent run. The transitional model gives a marked improvement, apparently capturing laminarization better.

The mesh sensitivity is tested with SST and run 445 as shown in figure 10. The sensitivity is low. Curiously enough, the crudest mesh is closest to the measurements. One plausible explanation is that the crude mesh smooths out the gradient normal to the wall, leading to a more laminar-like profile. Figure 10 also contains a comparison with results from CFX. Apart from different model implementations in the two codes, that simulation is different from the

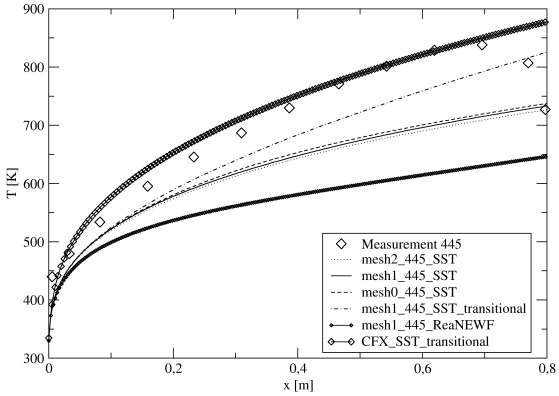

Figure 10. Heated wall temperature 445

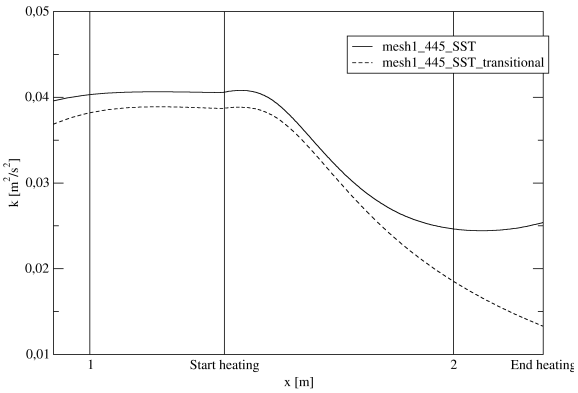

Figure 11. Axis turbulence kinetic energy

Fluent simulations in the mesh and fluid models. It gives a better match between simulations and measurements, but the qualitative behavior is also different, with a stronger temperature rise in the beginning. The reason for this remains to be investigated.

Figure 11 shows the turbulence kinetic energy, k, along the symmetry axis for the laminarizing run, 445. The turbulence kinetic energy decreases both with ordinary SST and SST with transition modeling, indicating that both models are able to capture some laminarization. However, with the transitional model, k continues to decrease through the whole channel. In the same figure, it can also be seen how k has reached a steady value before the entrance of the heated section and that the turbulence is somewhat weaker already at the inlet with the transitional model.

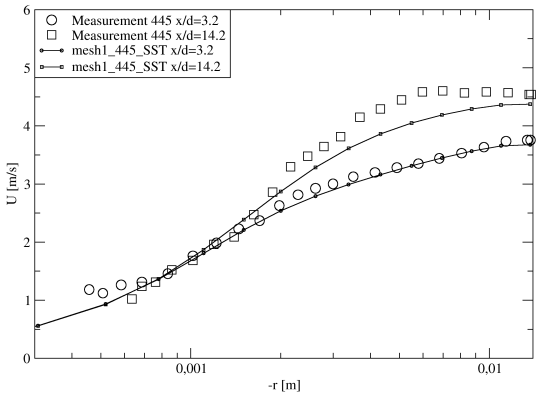

Figure 12. Mean axial velocity for case 445 at two first sections

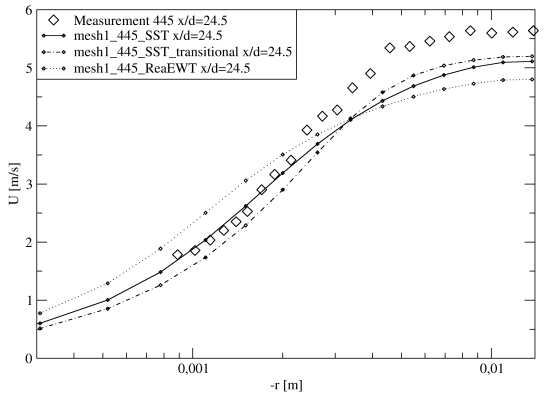

Figure 13. Mean axial velocity for case 445 at the last section

Figure 12 shows the axial velocity at two sections downstream of the start of the heated section, $x/d = 3.2 \approx 0.087m$ and $x/d = 14.2 \approx 0.39m$. It can be seen that the velocity profile matches well at the first section, close to the inlet, except closest to the wall. This may however

be due to reasons in the experiments, because the velocity goes to zero when approaching the wall. For the second section, the match is good at the wall, but there is some difference in the channel. This corresponds to the difference in temperature prediction due to the underprediction of the laminarization, seen also in figure 10.

Figure 13 shows the axial velocity at a section downstream of the start of the heated section, $x/d = 24.5 \approx 0.67m$. It can be seen how the transitional model improves the prediction, changing the shape of the typical more flat turbulent profile, in the direction of the typical parabolic laminar profile. It can also be seen how the Realizable model gives an even more flat profile.

4. Conclusions

The comparisons for these two test cases show that the tools can model the requested phenomena, natural convection, radiation and laminarization reasonably within the tested regime. There are some deviations and sensitivities that will be further investigate though, for example radiation boundary conditions/emissivity and turbulence transition.

Acknowledgements

Thanks to François Plewinski and Jörg Wolters for valuable input during different parts of this work.

References

[1] Kharoua C, Sabbagh P, Nilsson P, Mezei F, Plewinski F, Noah E, Sievers P, Zanini L, Takibayev A, Kecskes S, Ghidersa B E, Chen Y, Densham C, Sordo F and Magan M 2012 *Presented at ICANS XX*

[2] Inaba Y, Zhang Y, Takeda T and Shiina Y 2005 *Heat Transfer - Asian Research* **34** 293

[3] Shehata A M and McEligot D M 1995 *Turbulence structure in the viscous layer of strongly heated gas flows* vol INEL-95/0223 (Idaho National Engineering Laboratory)

[4] Shehata A M and McEligot D M 1998 *Int. J. Heat and Mass Transfer* **41** 4297

[5] Gordeev S, Heinzel V and Slobodtchouk V 2005 *Int. J. Heat and Mass Transfer* **48** 3363